Geophysical Research Letters

RESEARCH LETTER
10.1029/2018GL080483

On the Role of Dust-Climate Feedbacks During the Mid-Holocene

Peter O. Hopcroft[1] **and Paul J. Valdes**[2]

[1]School of Geography, Earth & Environmental Sciences, University of Birmingham, Birmingham, UK, [2]Bristol Research Initiative for the Dynamic Global Environment, School of Geographical Sciences, University of Bristol, Bristol, UK

Key Points:
- Dust was previously shown to reconcile GCM and proxy rainfall anomalies for mid-Holocene North Africa
- We use GCM simulations to show dependence on dust properties, a more realistic configuration shows no rainfall amplification
- This motivates a focus on the land surface and atmospheric convection response in this region

Supporting Information:
- Supporting Information S1

Correspondence to:
P. O. Hopcroft,
p.hopcroft@bham.ac.uk

Citation:
Hopcroft, P. O., & Valdes, P. J. (2019). On the role of dust-climate feedbacks during the mid-Holocene. *Geophysical Research Letters*, *46*, 1612–1621. https://doi.org/10.1029/2018GL080483

Received 14 SEP 2018
Accepted 19 DEC 2018
Accepted article online 27 DEC 2018
Published online 4 FEB 2019

Abstract A reduction in dust over North Africa during the mid-Holocene "Green Sahara" period could have amplified precipitation, helping reconcile climate model simulations with paleo-precipitation reconstructions. Here we test this using general circulation model simulations including interactive dust. We calculate a dust-precipitation amplification factor using three different dust configurations to evaluate the sensitivity to dust optical properties and particle size range. The resultant amplification ranges from −20% to 50%. With more absorbing dust properties, there is a large negative net radiative effect and hence a larger impact on the hydrological cycle. With the inclusion of particles greater than 1 μm in radius, the precipitation amplification is reversed. Based on the simulations which best match observed Saharan dust properties, we conclude that there was a limited enhancement of precipitation due to reduced dust during the mid-Holocene, meaning other aspects of the climate system should be the focus of future research.

Plain Language Summary From around 11,000–4,000 years ago, the area that is the modern day Sahara desert was covered in vegetation—the "Green" Sahara. This was brought about by long-term variations in the orbit of the Earth and the resultant changes in the distribution of incoming sunlight. However, when this period is simulated with climate models, the simulated rainfall increase is not adequate to maintain vegetation. We also know that this time period showed much reduced atmospheric dust from the desert. Here we study the effect of this dust reduction using a coupled climate-dust model. We find that the reduction in dust had little impact on rainfall change, because dust has opposing effects on heat and radiation in the atmosphere that approximately balance over North Africa. To understand this response, we configured different versions of our climate-dust model and show that the result is highly dependent on the physical characteristics of the dust particles that are given to the model. With the more realistic and up to date measurements from Saharan particles, the rainfall feedback is small. This means that future research needs to focus on rainfall processes in the atmosphere to better understand this "Greening" of the Sahara.

1. Introduction

During the early- to mid-Holocene, today's Sahara desert was mostly replaced by an area with vegetation (Hély et al., 2014; Lezine, 2017), lakes (Kohfeld & Harrison, 2000), and human and animal habitation (Dunne et al., 2012). Ultimately, this profound environmental conversion was forced by well-understood variations in the orbit of the Earth. This caused an intensification of the seasonal cycle of insolation in the northern hemisphere, though with little change in the insolation summed over a calendar year.

A summer insolation increase is thought to enhance monsoon circulations and precipitation (Joussaume et al., 1999; Kutzbach & Otto-Bliesner, 1982), but a number of feedbacks are also invoked to explain the amplitude of change during the early to mid-Holocene (Claussen et al., 2017). These include land surface and vegetation change (Braconnot et al., 1999; Coe & Bonan, 1997; Krinner et al., 2012) and ocean feedbacks (Braconnot et al., 1999). In response to a change in the orbital configuration, almost all general circulation models (GCMs) fail to reproduce the inferred amplitude of precipitation increase (Harrison et al., 2015; Perez-Sanz et al., 2014; Tierney et al., 2017). This may be because of weaknesses in dynamic vegetation schemes (Hopcroft et al., 2017) or because of more fundamental atmospheric dynamics. Only a few simulations (Claussen & Gayler, 1997; Egerer et al., 2016), some with large surface albedo changes (e.g., Levis et al., 2004; Pausata et al., 2016; Skinner & Poulsen, 2016), reproduce a stronger response, although in general the

latitudinal pattern does not match that inferred from pollen, with too much precipitation at around 10° N and not enough further north (Egerer et al., 2016; Pausata et al., 2016).

Desert dust is a key component in north Africa that has received relatively little attention in terms of Holocene climate change. Today, the Sahara is the single largest source of mineral dust on the planet (Huneeus et al., 2011). During the early to mid-Holocene, marine core sediment records show a 60–80% decline in dust deposition within around 100 km of the west African coast (deMenocal et al., 2000; McGee et al., 2013) and a similar reduction as far as the mid-Atlantic ridge (Middleton et al., 2018) and the Bahamas (Williams et al., 2016). This reduction in the Atlantic dust was probably caused by increased land surface coverage from vegetation and lakes (Egerer et al., 2016).

Pausata et al. (2016) and Gaetani et al. (2017) proposed that a large reduction in tropospheric dust during the mid-Holocene over north Africa would have enhanced the Saharan heat low, thus drawing the west African monsoon further north. In the model used, EC-Earth, a prescribed 80% reduction in dust aerosol optical depth (AOD) together with a prescribed vegetated Sahara, forced a precipitation increase of more than 50 mm or up to 50% at 20–30°N, relative to only changing the vegetation. Such an amplification would help to reconcile model simulations with reconstructed precipitation anomalies and would be an important step forward in understanding past monsoon dynamics in the region.

However, different models have different size ranges of dust particles and different optical properties (Huneeus et al., 2011; Kok, 2011; Miller et al., 2014), as compared in supporting information Table S1 (Chin et al., 2002; Kopke et al., 1997; Lau et al., 2009; Miller et al., 2004; Patterson, 1981; Patterson et al., 1977; Sinyuk et al., 2003; Sokolik et al., 1993; Solmon et al., 2008; Volz, 1973; Woodward, 2001; Yoshioka et al., 2007; Zakey et al., 2006). Many of these models are outside the range of more recent observations, which are also summarized in Table S1 (Haywood et al., 2003; Kim et al., 2011; McConnell et al., 2010; Patterson et al., 1977; Ryder et al., 2013; Sinyuk et al., 2003; Todd et al., 2007). There are also large uncertainties surrounding the representation of atmospheric convection and the land surface in North Africa (e.g., James et al., 2018; Vellinga et al., 2016; Vogel et al., 2018).

Here we employ an Earth System model (HadGEM2-ES) to quantify the role of dust as a feedback process for monsoon enhancement and warmth during the mid-Holocene. This model includes a fully interactive dust cycle that resolves interactive emissions, transport and deposition processes, and dust-radiation interactions. We report simulations of the preindustrial and mid-Holocene with and without a prescribed vegetated north Africa. In order to compare results from HadGEM2-ES with other models, we additionally test the role of different dust particle size ranges and dust optical properties (e.g., Miller et al., 2014). We use paired simulations with dust-radiative effects disabled to quantify the climatic influence of dust in the model.

2. Methods

2.1. GCM and Coupled Dust Scheme

We employ an atmosphere-only configuration of HadGEM2-ES (Collins et al., 2011; HadGEM2 Development Team, 2011). HadGEM2-ES has a horizontal resolution in the atmosphere of 1.875° × 1.25° with 38 unequally spaced vertical levels, 11 of which are above 15 km. It uses a semi-Lagrangian nonhydrostatic dynamical core (Martin et al., 2006). Land surface processes are simulated with an updated version of the Met Office Surface Exchange Scheme (Essery et al., 2003), which is coupled to a dynamic dust model, which represents emissions and transport and deposition, as well as the direct and semidirect radiative effects (Bellouin et al., 2011; Woodward, 2011). The HadGEM2-ES dust cycle has been configured based on observations from north Africa (Bellouin et al., 2011) and has been analyzed in detail for present day (Fiedler et al., 2016) and last glacial maximum conditions (Hopcroft et al., 2015). It simulates particle sizes in six classes up to a radius of 31.6 μm with radiative properties from Balkanski et al. (2007). A preferential source map is used (Woodward, 2011), but otherwise, emissions are a function of particle size-dependent threshold friction velocities, wind speed, soil moisture, and vegetation fraction.

In this work dynamic vegetation is disabled, and prescribed fields from observations are used for the preindustrial simulations. With this we use HadGEM2-AMIP dust parameters (Jones et al., 2011, their section 9.2) which give a larger dust flux per unit area of bare soil than in HadGEM2-ES. The lower dust emission efficiency in the latter is required to compensate for the overly expansive bare soil area simulated by the dynamic vegetation scheme. Our setup gives a much more realistic total and dust-only AOD over North Africa than that reported by Kim et al. (2014) for HadGEM2 (see Figure S1, Evan & Mukhopadhyay, 2010).

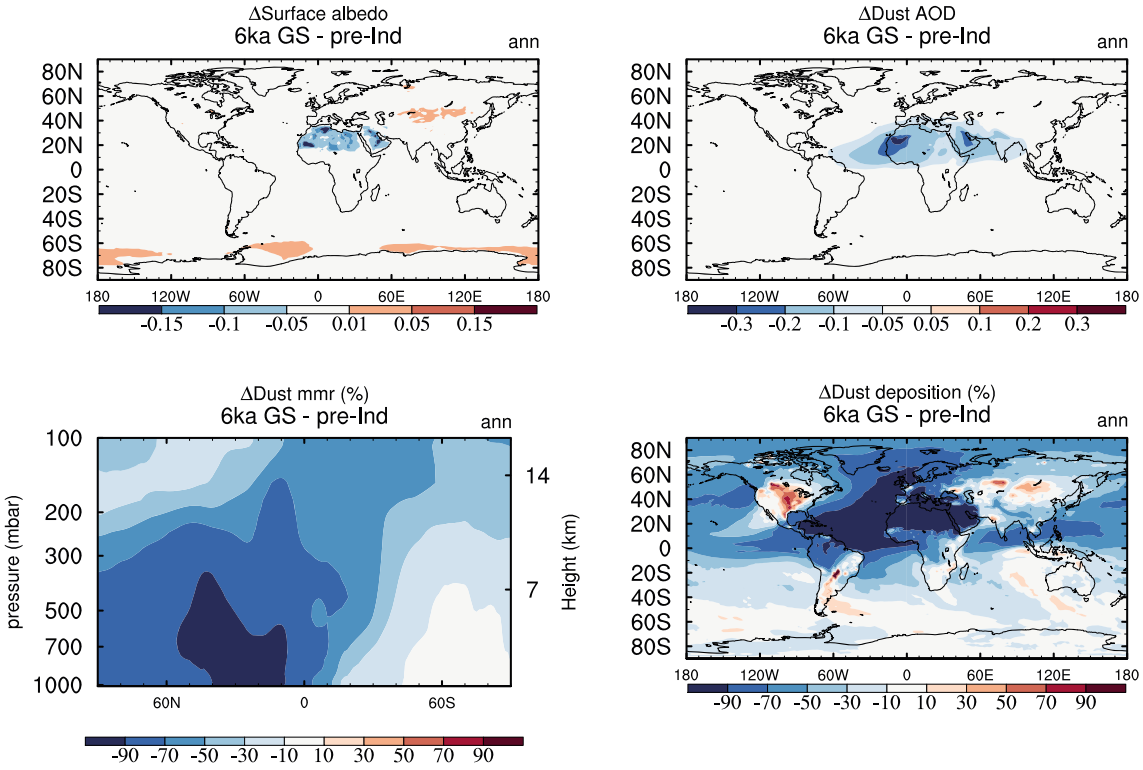

Figure 1. Response of the dust cycle to imposed "Greening" of the Sahara in mid-Holocene simulations with HadGEM2-ES relative to the preindustrial: (a) surface albedo change, (b) dust aerosol optical depth change (at 0.55 μm), (c) dust mass mixing ratio change (%) averaged from 30°W to 20°E, and (d) dust deposition change (%). See Table 1 for regional values and anomalies. AOD = aerosol optical depth.

We perform preindustrial simulations following Coupled Model Intercomparison Project phase 5 (CMIP5) boundary conditions (Jones et al., 2011). For the mid-Holocene, the orbital parameters are set to conditions for 6ka following the Paleoclimate Model Intercomparison Project Phase 3 (PMIP3) protocol, and the Sahara region is replaced with 100% grass coverage. This is referred to as "Green Sahara" or GS below. This is approximately equivalent to the simulations by Pausata et al. (2016) and the *midHolocene-veg* simulations described by Otto-Bleisner et al. (2017) for PMIP4. The vegetation coverage prevents any emissions of dust from this region in the model and is specifically designed to produce the largest theoretical change in dust and hence in dust-climate effects. Sea surface temperatures (SSTs) and sea ice in both cases use a climatology from HadISST from the years 1871–1900. These are not meant to be realistic for the mid-Holocene but are chosen to simplify the analyses. Greenhouse gases are not modified for the mid-Holocene because the reduction in radiative forcing is too small to appreciably alter precipitation (Otto-Bleisner et al., 2017).

To further understand the role of different-sized particles, we ran HadGEM2-ES using radiative properties for dust similar to Deepak and Gerber (1983). These values are more absorbing than the default model which are derived from Balkanski et al. (2007). Second, this model version is configured with dust particles only in the three smaller size bins (<1μm) in order to mimic other GCMs which have a limited dust particle size range. All simulations are atmosphere-only and are 30 years in length. All model years are used to calculate climatologies. These simulations are listed in Table S2. According to the results of several field campaigns listed in Table S1, the HadGEM2-ES configuration has the most realistic dust optical properties and size distribution for North Africa. The other two model configurations tested here are similar to some earlier modeling studies, in having too high a value of the complex refractive index.

3. Results

3.1. Dust Cycle Response

The dust cycle response to the combination of both 6ka orbital parameters and a Green Sahara in HadGEM2-ES is shown in Figure 1 and is summarized in Table 1. The surface albedo averaged over North Africa (20–30°N) reduces from 0.34 to 0.26. The dust AOD at 0.55 μm reduces from 0.20 to 0.01 averaged

Table 1
Annual-Mean Simulated Changes in Dust Cycle and Precipitation Over North Africa (20–30°N, 20°E–20°W)

Simulation	Loading (Tg)	DAOD	Surface albedo	Precipitation (mm/day)
HadGEM2-ES				
0ka	1.6	0.20	0.34	0.07
0ka*	1.4	—	0.34	0.07
6ka	2.0	0.26	0.34	0.08
$6ka_{GS}$	0.0	0.01	0.26	0.20
$6ka_{GS}^{PD}$	2.1	0.18	0.26	0.20
$6ka_{GS}$*	0.0	—	0.26	0.20
HadGEM2-ES-DG83				
0ka	1.6	0.23	0.34	0.07
$6ka_{GS}$	0.0	0.01	0.26	0.20
HadGEM2-ES-DG83 <1 μm				
0ka	0.6	0.22	0.34	0.07
6ka	0.6	0.25	0.34	0.08
$6ka_{GS}$	0.0	0.01	0.26	0.21
$6ka_{GS}^{PD}$	0.6	0.21	0.26	0.18

Note. DAOD is dust aerosol optical depth at 0.55 μm. ^{PD} indicates pre-industrial dust in a mid-Holocene simulation. This is approximated as described in the text.
*Dust-radiative effects are set to zero; dust is a passive tracer.

over the same region. There is a 90% reduction in dust loading over most of North Africa and the equatorial Atlantic. The dust aerosol layer is reduced by around 80% up to approximately 10 km over most of the northern hemisphere in the longitudinal zone from 30°W to 20°E.

Overall, the complete removal of the north African dust source results in an overly strong reduction of the dust cycle compared with marine proxy reconstructions (e.g., as compiled by Egerer et al., 2016, in their table 5, and references therein), but it does serve as an idealized scenario with which to understand the underlying mechanisms affecting the regional climate.

3.2. Dust-Hydrological Cycle Interactions

The relative change in precipitation is calculated as the anomaly relative to paired identical simulations in which dust-radiative effects are deactivated. That is,

$$\Delta P_1 = \Delta P(6k) - \Delta P(0k) = P_{6kaGS} - P^*_{6kaGS} - (P_{0ka} - P^*_{0ka}), \quad (1)$$

where * indicates that dust-radiation interactions are deactivated and GS indicates a vegetated Sahara. Simulations without dust-radiation effects are only performed for the HadGEM2-ES simulation as the prescribed dust optical properties and size range no longer have any influence on the simulated climate.

The percentage change in this anomaly relative to these dust-off simulations are shown in Figure 2. The three curves are for the default HadGEM2-ES (HadGEM2-ES), the version using more absorbing dust optical properties (HadGEM2-ES-DG83), and this version with only smaller particles included (HadGEM2-ES-DG83 $< 1\ \mu$m).

North of 10°N, the precipitation amplification is mostly at the 10% level or less. The HadGEM2-ES-DG83 and HadGEM2-ES-DG83 <1 μm versions are different. The HadGEM2-ES-DG83 version shows an attenuation of precipitation by dust, whereas the HadGEM2-ES-DG83 <1 μm shows a larger effect than the standard version (HadGEM2-ES). The peak is around 15% at 30°N.

The atmospheric heating impacts in the preindustrial HadGEM2-ES model versions are compared in Figure S2. This shows that HadGEM2-ES has the weakest long-wave cooling in the atmosphere, while the short-wave heating is the largest in HadGEM2-ES-DG83. More absorbing optical properties in HadGEM2-ES-DG83 significantly enhance the negative surface short-wave (SW) and hence net forcing. Omitting the larger particles in HadGEM2-ES-DG83 $< 1\ \mu$m mostly retains the positive long-wave (LW) surface radiative forcing but also slightly reduces the SW term. Overall, the net surface forcing is most

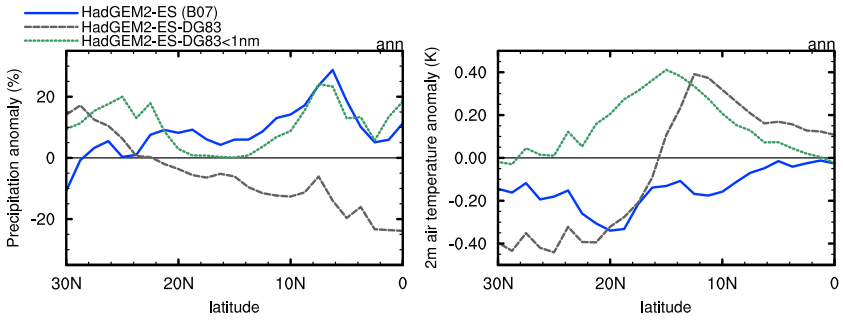

Figure 2. Relative change (%) in the zonal mean (20°W–30°E) and annual mean mid-Holocene minus preindustrial precipitation and surface air temperature anomaly over North Africa. Anomalies are relative to a control pair of simulations with no dust-radiation effects, that is, $\Delta P_1/(P^*_{6\text{kaGS}} - P^*_{0\text{ka}})$, where ΔP_1 is defined by equation (1). Shown are the three model versions described in the text. All simulations use the same preindustrial SST fields.

negative in the HadGEM2-ES-DG83 case and is much closer to a balance between SW and LW terms in HadGEM2-ES.

These radiative forcing changes have the most impact on the preindustrial because dust loading in the 6kaGS is close to zero. In all preindustrial simulations, precipitation over the Sahara is close to zero, and different dust schemes make little difference in this arid region. The HadGEM2-ES-DG83 run simulates enhanced precipitation as a result of the inclusion of dust by around 10%. This is because it has the strongest negative radiative forcing at the surface and a dominant heating term in the atmospheric column. Although heating aloft and cooling at the surface will stabilize the column, Lau et al. (2009) showed that it can also promote inflow of moisture from the Atlantic, increasing precipitation across West Africa. This leads to positive humidity anomalies in lower troposphere and a small strengthening of the Africa Easterly Jet (Figure S3). The humidity and temperature terms in the moist static energy budget are dominant (Figure S4). A similar picture but with weaker heating changes emerges in the HadGEM2-ES-DG83 <1 μm model, and only a weak cooling at the surface is simulated in HadGEM2-ES. These two model configurations show lower humidity and almost no change to the large-scale circulation (Figures S3 and S4) and are both drier as a result of dust for the preindustrial. Thus, the balance of different processes (e.g., Solmon et al., 2008) is altered by differing dust-radiative properties among these model versions. The inclusion of dust also impacts precipitation in the 6kaGS simulations (i.e., relative to the no dust 6kaGS simulations), but the magnitude of the anomalies is small because the dust loading over the Sahara is significantly reduced (e.g., Figure 1).

Pausata et al. (2016) calculate the precipitation effect slightly differently, as the difference between 6kaGS with reduced and pre-industrial (0 ka) dust loading:

$$\Delta P_2 = P_{6\text{kaGS}} - P^{\text{PD}}_{0\text{ka}} - \left[P^{\text{PD}}_{6\text{kaGS}} - P^{\text{PD}}_{0\text{ka}}\right] = P_{6\text{kaGS}} - P^{\text{PD}}_{6\text{kaGS}}, \quad (2)$$

where GS signifies a vegetated or Green Sahara, PD signifies pre-industrial dust, and 0ka or 6ka refer to orbital parameters in the climate simulation. If PD is not specified, then the simulation has interactive dust. Since dust is coupled to the land surface in HadGEM2-ES, it is not possible to perform a 6kaGS simulation with pre-industrial dust loading, that is, 6kGS^{PD} in equation (2). Instead, we modified HadGEM2-ES to allow dust emissions where vegetation is present over the Sahara and ran this model version with 6ka orbital parameters and a fully vegetated Sahara, thus giving an approximation of 6kGS^{PD}. For this, it is necessary to adjust the wind threshold parameter to account for the impact of vegetation on boundary layer wind speeds (only over the Sahara). The resultant dust AOD is within 0.02 of the equivalent preindustrial simulations (as compared in Table 1 and Figures S5 and S6).

The resultant $\Delta P2$ calculations are shown in Figure 3 for the HadGEM2-ES and HadGEM2-ES-DG83 <1 μm model versions. The latter shows a very similar percentage amplification of the precipitation anomaly over North Africa as in the results of Pausata et al. (2016), linearly increasing to 50% by around 25–30°N. The default HadGEM2-ES model configuration (HadGEM2-ES) shows less precipitation amplification North of 10°N.

The EC-Earth model version is equivalent to the HadGEM2-ES-DG83 <1 μm version, because both models use similar optical properties (from Hess et al., 1998 and DG83) and have a similar dust size range (<0.90 μm

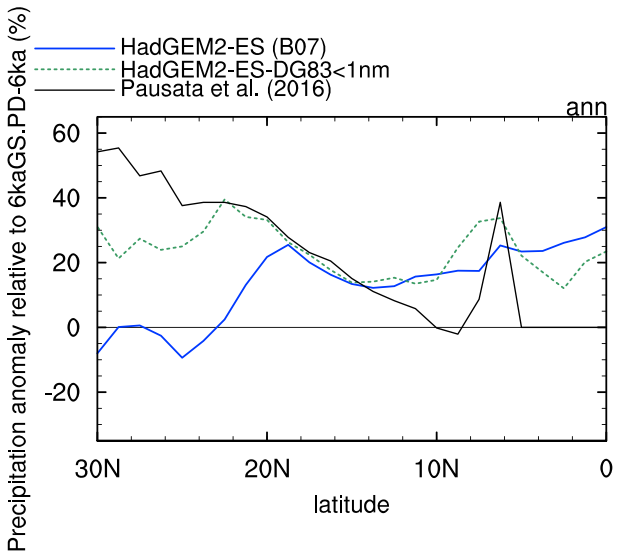

Figure 3. As in Figure 2 but showing the percentage difference in the $6ka_{GS}$ − 6ka precipitation anomaly relative to $6ka^{PD}_{GS}$ − 6ka anomaly, that is, ΔP_2, defined by equation (2). Also, shown is the percentage difference in the precipitation anomaly digitized from Figure 2 by Pausata et al. (2016), as a result of imposing an 80% dust reduction and a vegetated Sahara.

for EC-Earth and <1 nm). This similarity is borne out by the precipitation responses compared in Figure 3. This indicates that dust optical property assumptions can be crucial for understanding the dust-climate feedbacks in different GCMs.

The difference in the dust-precipitation effect calculations (equations (1) and (2)) is due to the effect of surface albedo change. Comparing preindustrial or 6kaGS simulations with and without dust will not show any precipitation change over the northern Sahara. For 6kaGS − 6kaGS*, the dust effects are effectively zero due to the very low dust loading, while for the preindustrial, the precipitation is nearly zero in this zone, irrespective of dust effects. When dust is allowed over vegetated land surface, the radiative impacts are much stronger because of the albedo contrast between the vegetated land surface and the aerosol layer (as discussed by Pausata et al., 2016). Hence, the diagnosed precipitation effect of dust is much larger using equation (2) and could be thought of as an indirect radiative forcing by the land-surface change.

In both cases, however, the HadGEM2-ES dust properties lead to much smaller-diagnosed dust-precipitation effects. In equation (2), this is because HadGEM2-ES has a weaker SW forcing at the surface and a larger compensatory LW forcing (Figure 4). Since HadGEM2-ES dust properties are based on observations over the Sahara, whereas the more absorbing HadGEM2-ES-DG83 properties have overly high complex refractive indices (Balkanski et al., 2007; Haywood et al., 2003; Kim et al., 2011; McConnell et al., 2010), we conclude that the dust impact on precipitation is likely substantially smaller than estimated by Pausata et al. (2016), that is, closer to the HadGEM2-ES model results.

3.3. Dust Direct Radiative Forcing

Dust-radiative forcing could also impact the global mean temperature as well as the SST gradient in the North Atlantic, thereby indirectly influencing precipitation over North Africa. The net downward radiative flux anomalies due to dust between the preindustrial and mid-Holocene are shown in Figure 4. The standard HadGEM2-ES configuration shows a net warming effect over the tropical Atlantic but only by 3–7 Wm^{-2}. This increases substantially with the DG83 dust optical properties, but as noted above, these are likely unrealistic for Saharan dust.

Y. Liu et al. (2018) have suggested that dust may have contributed to Holocene temperature conundrum (e.g., see Z. Liu et al., 2014), since less dust exported to the northern hemisphere from a vegetated Sahara will lead to a surface warming relative to the preindustrial. Our simulations support this mechanism to some extent but also highlight the substantial contribution from LW effects, which were not included in the model results of Y. Liu et al. (2018). LW effects act to oppose the warming and are substantial close to the dust source regions (Kok et al., 2017), such as in the Eastern equatorial Atlantic. Moreover, it has been shown that the Holocene thermal maximum has the strongest expression north of 30°N in the North Atlantic (Marsicek et al., 2018), which is not a region of particularly strong dust-radiative forcing in any of our simulations. Hence, the explanation for this signal during the mid-Holocene may require other mechanisms.

4. Discussion

In nature, the true dust particle size distribution may be coarser than in most models (Kok, 2011), so that the ability of dust to absorb solar radiation is even stronger than simulated in HadGEM2-ES (Kok et al., 2017). These larger particles have a shorter lifetime and are hence more important closer to dust source regions, such as over the Sahara (Mahowald et al., 2014; Ryder et al., 2013). Comparing HadGEM2-ES-DG83 with HadGEM2-ES-DG83 <1 μm in Figure 2, we see that the larger particles modify the overall dust-precipitation feedback to be negative. Thus, we suggest that inclusion of a larger tail of heavier dust particles may further weaken the dust feedback at the mid-Holocene. Furthermore, the majority of models, including HadGEM2-ES, neglect LW scattering effects (Dufresne et al., 2002), which could further amplify the long-wave effects, and therefore further offset SW effects.

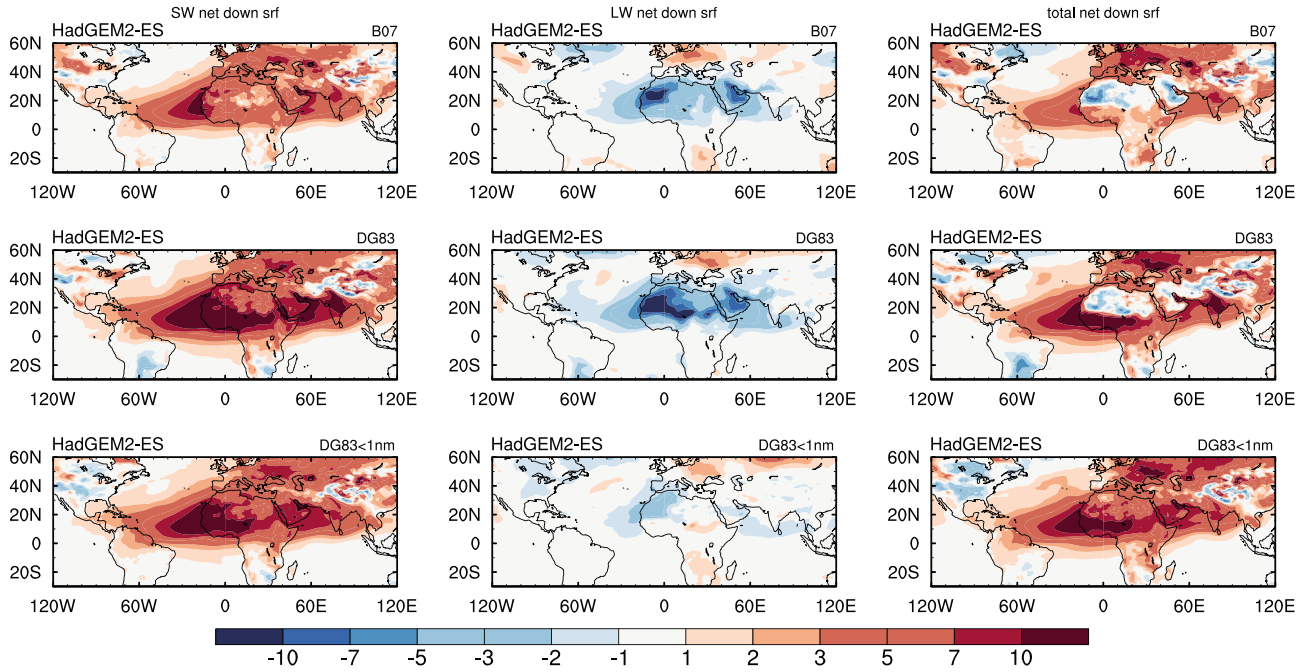

Figure 4. Surface net radiative flux change (Wm^{-2}), 6kaGS minus preindustrial, for SW, LW, and total (SW + LW) due to mineral dust.

The radiative forcing over the tropical Atlantic could have modulated precipitation in North Africa according to mechanisms previously diagnosed from historical period (e.g., Folland et al., 1986; Hoerling et al., 2006). However, Yoshioka et al. (2007) estimated that this indirect SST-precipitation feedback from dust is smaller than the direct impact of dust on the atmospheric radiation balance. The radiative forcing of dust over the darker ocean surface is generally negative as larger particles with a strong LW forcing are preferentially lost. Hence, the influence on the SST field may be less model dependent than over desert surface (e.g., see Figure 4). We leave a full evaluation of this to future work.

Dust-cloud interactions are only just being included in global models (e.g., Sagoo & Storelvmo, 2017). These may also be important in this region, as shown by relatively strong precipitation changes reported for idealized low and high dust simulations by Sagoo and Storelvmo (2017). New simulations with a more sophisticated dust scheme are required to evaluate these effects and their associated uncertainties.

The simulated dust deposition field over the Atlantic reduces by around 90–100% (Figure 1), whereas sedimentary records show a more modest 40–85% reduction (Egerer et al., 2016; Middleton et al., 2018; Williams et al., 2016). Hence, the overall experimental design employed here is probably overestimating the reduction in bare soil in the region. However, it is not feasible to derive a percentage vegetation coverage from pollen data (Hély et al., 2014; Lezine, 2017), and the dynamic vegetation scheme in HadGEM2-ES tends to simulate overly polarized coverage (i.e., tending to zero or 100%), which is another reason that dynamic vegetation was not used in this study. In reality, the impact of a reduced dust loading on the hydrological cycle may have been even weaker than our model simulations suggest. This lends further support to the main conclusions of this study.

The soil albedo probably also changed as a result of vegetation growth and associated litterfall. We have not accounted for this in HadGEM2-ES. Several schemes have been developed, and these allow the surface albedo to change as a function of vegetation coverage (e.g., Vamborg et al., 2011), which is critical for the effective radiative forcing by dust (Pausata et al., 2016).

5. Conclusions

We used a GCM HadGEM2-ES which includes an interactive mineral dust cycle to test the role of dust-radiative forcing in the precipitation increase over North Africa during the mid-Holocene. We used three different model configurations of the dust cycle to evaluate the influence from resolved particle size

distribution and optical properties to characterize uncertainty and compare with other studies. With more absorbing dust optical properties (Deepak & Gerber, 1983) and a size range limited to 1 μm, the simulated precipitation amplification closely replicates results from the GCM EC-Earth (Pausata et al., 2016), as shown in Figure 3, showing up to 50% amplification of the precipitation signal over North Africa. This demonstrates that dust cycle properties are crucial for understanding the real system. However, including a larger particle size range (<33 μm) reverses the sign of the precipitation feedback, so that dust reduces the precipitation during the mid-Holocene.

With the default HadGEM2-ES dust properties (Bellouin et al., 2011), the dust-precipitation feedback is limited north of 10°N. This is because this simulation shows weaker SW forcing at the surface but also much larger compensatory LW forcing, which is more important close to source regions like the Sahara (e.g., Kok et al., 2017). This latter simulation is in best agreement with observations of Saharan dust both in terms of the absorption properties (Balkanski et al., 2007; Haywood et al., 2003; Kim et al., 2011; McConnell et al., 2010) and the size distribution over land (Ryder et al., 2013), so we conclude that dust did not significantly enhance precipitation in North Africa during the mid-Holocene.

Instead, other mechanisms or uncertainties within the climate system of North Africa are required to explain the full magnitude of precipitation increase at this time. Given that our simulations already include a fully vegetated land surface, we suggest that the atmospheric response is too weak. Synoptic systems in this region are poorly resolved in global GCMs (e.g., Vellinga et al., 2016; Vogel et al., 2018), so atmospheric convection is an obvious choice for further research. Future work on the dust cycle should use common sets of dust optical properties in different GCMs as well as incorporating dust-cloud interactions to further understand intermodel differences in dust-climate interactions and to better understand the full role that mineral dust plays in the climate system. However, the influence of surface albedo change is also important, and this is crudely estimated in many studies to date.

Acknowledgments
P. O. H. is supported by a University of Birmingham fellowship. This work was carried out on the UK National HPC facility ARCHER (http:/www.archer.ac.uk). We thank G. Lister (NCAS) for help with configuring the HadGEM2 simulations. We thank S. Woodward (UK Met Office) for advice on dust physical properties in the UM. The source code for UK Met Office Unified Model is subject to Crown Copyright. It is available for use under license, see http://www.metoffice.gov.uk/research/collaboration. Model output is available for further analysis from http://www.bridge.bristol.ac.uk/resources/simulations.

References

Balkanski, Y., Schulz, M., Claquin, T., & Guibert, S. (2007). Reevaluation of mineral aerosol radiative forcings suggests a better agreement with satellite and AERONET data. *Atmospheric Chemistry and Physics*, *7*, 81–95.

Bellouin, N., Rae, J., Jones, A., Johnson, C., Haywood, J., & Boucher, O. (2011). Aerosol forcing in the CMIP5 simulations by HadGEM2-ES and the role of ammonium nitrate. *Journal of Geophysical Research*, *116*, D20206. https://doi.org/10.1029/2011JD016074

Braconnot, P., Joussaume, S., Marti, O., & de Noblet, N. (1999). Synergistic feedbacks from ocean and vegetation on the African monsoon response to mid-Holocene insolation. *Geophysical Research Letters*, *26*(16), 2481–2484. https://doi.org/10.1029/1999GL006047

Chin, M., Ginoux, P., Kinne, S., Torres, O., Holben, B. N., Duncan, B. N., et al. (2002). Tropospheric aerosol optical thickness from the GOCART model and comparisons with satellite and sun photometer measurements. *Journal of the Atmospheric Sciences*, *59*, 461–483.

Claussen, M., Dallmeyer, A., & Bader, J. (2017). Theory and modeling of the African humid period and the Green Sahara. *Oxford research encyclopedia of climate science* (pp. 1–38). New York: Oxford University Press. https://doi.org/10.1093/acrefore/9780190228620.013.532

Claussen, M., & Gayler, V. (1997). The greening of the Sahara during the mid-Holocene: Results of an interactive atmosphere-biome model. *Global Ecology and Biogeography Letters*, *6*(5), 369–377.

Coe, M., & Bonan, G. (1997). Feedbacks between climate and surface water in northern Africa during the middle Holocene. *Journal of Geophysical Research*, *102*, 11,087–11,101.

Collins, W., Bellouin, N., Doutriaux-Boucher, M., Gedney, N., Halloran, P., Hinton, T., et al. (2011). Development and evaluation of an earth-system model–HadGEM2. *Geoscientific Model Development*, *4*, 1051–1075. https://doi.org/10.5194/gmd-4-1051-2011

deMenocal, P., Ortiz, J., Guilderson, T., Adkins, J., Sarnthein, M., Baker, L., & Yarusinsky, M. (2000). Abrupt onset and termination of the African humid period: Rapid climate responses to gradual insolation forcing. *Quaternary Science Reviews*, *19*, 347–361.

Deepak, A., & Gerber, H. E. (1983). *Report of the experts' meeting on aerosols and their climatic effects (28-30 March 1983; Williamsburg, United States)*. Geneva, Switzerland: World Meteorological Organization.

Dufresne, J.-L., Gautier, C., & Fouquart, Y. (2002). Long-wave scattering of mineral aerosols. *Journal of Atmospheric Sciences*, *59*, 1959–1966.

Dunne, J., Evershed, R., Salque, M., Cramp, L., Bruni, S., Ryan, K., et al. (2012). First dairying in Green Saharan Africa in the fifth millennium BC. *Nature*, *486*, 390–394.

Egerer, S., Claussen, M., Reick, C., & Stanelle, T. (2016). The link between marine sediment records and changes in Holocene Saharan landscape: Simulating the dust cycle. *Climate of the Past*, *12*, 1009–1027. https://doi.org/10.5194/cp-12-1009-2016

Essery, R., Best, M., Betts, R., Cox, P., & Taylor, C. (2003). Explicit representation of subgrid heterogeneity in a GCM land-surface scheme. *Journal of Hydrometeorology*, *4*, 530–543.

Evan, A., & Mukhopadhyay, S. (2010). African Dust over the Northern Tropical Atlantic: 1955-2008. *Journal of Applied Meteorology and Climatology*, *49*, 2213–2229. https://doi.org/10.1175/2010JAMC2485.1

Fiedler, S., Knippertz, P., Woodward, S., Martin, G. M., Bellouin, N., Ross, A. N., et al. (2016). A process-based evaluation of dust-emitting winds in the CMIP5 simulation of HadGEM2. *Climate Dynamics*, *46*, 1107–1130. https://doi.org/10.1007/s00382-015-2635-9

Folland, C., Palmer, T., & Parker, D. (1986). Sahel rainfall and worldwide sea temperatures 1901-1985. *Nature*, *320*, 602–607.

Gaetani, M., Messori, G., Zhang, Q., Flamant, C., & Pausata, F. S. R. (2017). Understanding the mechanisms behind the northward extension of the west African monsoon during the mid-Holocene. *Journal of Climate*, *30*, 7621–7643.

HadGEM2 Development Team (2011). The HadGEM2 family of Met Office Unified Model climate configurations. *Geoscientific Model Development*, *4*, 7233–757. https://doi.org/10.5194/gmd-4-723-2011

Harrison, S., Bartlein, P. J., Izumi, K., Li, G., Annan, J., Hargreaves, J., et al. (2015). Evaluation of CMIP5 palaeo-simulations to improve climate projections. *Nature Climate Change*, *5*, 735–743.

Haywood, J., Francis, P., Osborne, S., Glew, M., Loeb, N., Highwood, E., et al. (2003). Radiative properties and direct radiative effect of Saharan dust measured by the C-130 aircraft during SHADE: 1. Solar spectrum. *Journal of Geophysical Research*, *108*(D18), 8577. https://doi.org/10.1029/2002JD002687

Hély, C., Lezine, A.-M., & contributors, APD (2014). Holocene changes in African vegetation: Tradeoff between climate and water availability. *Climate of the Past*, *10*, 681–686. https://doi.org/10.5194/cp-10-681-2014

Hess, M., Koepke, P., & Schult, I. (1998). Optical properties of aerosols and clouds: The software package OPAC. *Bulletin of the American Meteorological Society*, *79*, 831–844.

Hoerling, M., HurrelL, J., Eischeid, J., & Phillips, A. (2006). Detection and attribution of 20th century northern and southern African rainfall change. *Journal of Climate*, *19*, 3989–4008.

Hopcroft, P., Valdes, P., Harper, A., & Beerling, D. (2017). Multi vegetation model evaluation of the Green Sahara climate regime. *Geophysical Research Letters*, *44*, 6804–6813. https://doi.org/10.1002/2017GL073740

Hopcroft, P., Valdes, P., Woodward, S., & Joshi, M. (2015). Last glacial maximum radiative forcing from mineral dust aerosols in an Earth system model. *Journal of Geophysical Research: Atmospheres*, *120*, 8186–8205. https://doi.org/doi:10.1002/2015JD023742

Huneeus, N., Schulz, M., Balkanski, Y., Griesfeller, J., Prospero, J., Kinne, S., et al. (2011). Global dust model intercomparison in AeroCom phase I. *Atmospheric Chemistry and Physics*, *11*, 7781–7816. https://doi.org/10.5194/acp-11-7781-2011

James, R., Washington, R., Abiodun, B., Kay, G., Mutemi, J., Pokam, W., et al. (2018). Evaluating climate models with an African lens. *Bulletin of the American Meteorological Society*, *99*(2), 313–336. https://doi.org/10.1175/BAMS-D-16-0090.1

Jones, C., Hughes, J., Bellouin, N., Hardiman, S., Jones, G., Knight, J., et al. (2011). The HadGEM2-ES implementation of CMIP5 centennial simulations. *Geoscientific Model Development*, *4*, 543–570.

Joussaume, S., Taylor, K. E., Braconnot, P., Mitchell, J. F. B., Kutzbach, J. E., Harrison, S. P., et al. (1999). Monsoon changes for 6000 years ago: Results of 18 simulations from the paleoclimate modeling intercomparison project (PMIP). *Geophysical Research Letters*, *26*(7), 859–862.

Kim, D., Chin, M., Diehl, T., Tan, Q., Kahn, R. A., Tsigaridis, K., et al. (2014). Sources, sinks, and transatlantic transport of North African dust aerosol: A multimodel analysis and comparison with remote sensing data. *Journal of Geophysical Research: Atmospheres*, *119*, 6259–6277. https://doi.org/10.1002/2013JD021099

Kim, D., Chin, M., Yu, H., Eck, T., Sinyuk, A., Smirnov, A., & Holben, B. (2011). Dust optical properties over North Africa and Arabian Peninsula derived from the AERONET dataset. *Atmospheric Chemistry and Physics*, *11*, 10,733–10,741.

Kohfeld, K., & Harrison, S. (2000). How well can we simulate past climates? Evaluating the models using palaeoenvironmental datasets. *Quaternary Science Reviews*, *19*, 321–346.

Kok, J. (2011). A scaling theory for the size distribution of emitted dust aerosols suggests climate models underestimate the size of the global dust cycle. *Proceedings of the National Academy of Sciences of the United States of America*, *108*(3), 1016–1021.

Kok, J., Ridley, D., Zhou, Q., Miller, R. L., Zhao, C., Heald, C. L., et al. (2017). Smaller desert dust cooling effect estimated from analysis of dust size and abundance. *Nature Geoscience*, *10*, 274–278. https://doi.org/10.1038/NGEO2912

Kopke, P., Hess, M., Schult, I., & Shettle, E. (1997). *Global aerosol data set*. Hamburg: MPI Hamburg.

Krinner, G., Lézine, A.-M., Braconnot, P., Sepulchre, P., Ramstein, G., Grenier, C., & Gouttevin, I. (2012). A reassessment of lake and wetland feedbacks on the North African holocene climate. *Geophysical Research Letters*, *39*, L07701. https://doi.org/10.1029/2012GL050992

Kutzbach, J., & Otto-Bliesner, B. (1982). The sensitivity of the African-Asian monsoonal climate to orbital parameter changes for 9000 year B.P. in a low-resolution general circulation model. *Journal of the Atmospheric Sciences*, *39*(6), 1177–1188.

Lau, K., Kim, K., Sud, Y., & Walker, G. (2009). A GCM study of the response of the atmospheric water cycle of West Africa and the Atlantic to Saharan dust radiative forcing. *Annales de Geophysique*, *27*, 4023–4037.

Levis, S., Bonan, G., & Bonfils, C. (2004). Soil feedback drives the mid-Holocene North African monsoon northward in fully coupled CCSM2 simulations with a dynamic vegetation model. *Climate Dynamics*, *23*, 791–802.

Lezine, A.-M. (2017). Vegetation at the time of the African humid period. *Oxford research encyclopedia of climate science* (pp. 1–28). Oxford: Oxford University Press. https://doi.org/10.1093/acrefore/9780190228620.013.530

Liu, Y., Zhang, M., Liu, Z., Xia, Y., Huang, Y., Peng, Y., & Zhu, J. (2018). A possible role of dust in resolving the Holocene temperature conundrum. *Scientific Reports*, *8*, 4434. https://doi.org/10.1038/s41598-018-22841-5

Liu, Z., Zhu, J., Rosenthal, Y., Zhang, X., Otto-Bliesner, B. L., Timmermann, A., et al. (2014). The Holocene temperature conundrum. *Proceedings of the National Academy of Sciences of the United States of America*, *111*, E3501–E3505.

Mahowald, N., Albani, S., Kok, J., Engelstaeder, S., Scanza, R., Ward, D., & Flanner, M. (2014). The size distribution of desert dust aerosols and its impact on the earth system. *Aeolian Research*, *15*, 53–71. https://doi.org/10.1016/j.aeolia.2013.09.002

Marsicek, J., Shuman, B., Bartlein, P., Shafer, S. L., & Brewer, S. (2018). Reconciling divergent trends and millennial variations in Holocene temperatures. *Nature*, *554*, 92–96. https://doi.org/10.1038/nature25464

Martin, G., Ringer, M. A., Pope, V. D., Jones, A., & Hinton, T. J. (2006). The physical properties of the atmosphere in the new Hadley Centre Global Environmental Model (HadGEM1). Part I: Model description and global climatology. *Journal of Climate*, *19*, 1274.

McConnell, C., Formenti, P., Highwood, E., & Harrison, M. (2010). Using aircraft measurements to determine the refractive index of Saharan dust during the DODO experiments. *Atmospheric Chemistry and Physics*, *10*, 3081–3098.

McGee, D., deMenocal, P., Winckler, G., Stuut, J., & Bradtmiller, L. (2013). The magnitude, timing and abruptness of changes in north African dust deposition over the last 20,000 yr. *Earth and Planetary Science Letters*, *371-372*, 163–176. https://doi.org/10.1016/j.epsl.2013.03.054

Middleton, J., Mukhopadhyay, S., Langmuir, C., McManus, J. F., & Huybers, P. J. (2018). Millennial-scale variations in dustiness recorded in mid-Atlantic sediments from 0 to 70ka. *Earth and Planetary Science Letters*, *482*, 1–20.

Miller, R., Knippertz, P., Garcia-Pando, C., Perlwitz, J., & Tegen, I. (2014). Impact of dust radiative forcing upon climate. In P. Knippertz & J.-B. Stuut (Eds.), *Mineral dust: A key player in the Earth system* (pp. 327–357), 13. Dordrecht: Springer Science+Business Media. https://doi.org/10.1007/978-94-017-8978-3_13

Miller, R., Tegen, I., & Perlwitz, J. (2004). Surface radiative forcing by soil dust aerosols and the hydrologic cycle. *Journal of Geophysical Research*, *109*, D04203. https://doi.org/10.1029/2003JD004085

Otto-Bleisner, B., Braconnot, P., Harrison, S., Lunt, D., Abe-Ouchi, A., Albani, S., et al. (2017). The PMIP4 contribution to CMIP6 part 2: Two interglacials, scientific objective and experimental design for holocene and last interglacial simulations. *Geoscientific Model Development*, *10*, 3979–4003.

Patterson, E. (1981). Optical properties of the crustal aerosol: Relation to chemical and physical characteristics. *Journal of Geophysical Research*, *86*, 3236–3246.

Patterson, E., Gillette, D., & Stockton, B. (1977). Complex index of refraction between 300 and 700 nm for Saharan aerosols. *Journal of Geophysical Research*, *82*, 3153–3160.
Pausata, F., Messori, G., & Zhang, Q. (2016). Impacts of dust reduction on the northward expansion of the African monsoon during the Green Sahara period. *Earth and Planetary Science Letters*, *434*, 298–307.
Perez-Sanz, A., Li, G., González-Sampériz, P., & Harrison, S. P. (2014). Evaluation of modern and mid-Holocene seasonal precipitation of the Mediterranean and northern Africa in the CMIP5 simulations. *Climate of the Past*, *10*, 551–568.
Ryder, C. L., Highwood, E. J., Rosenberg, P. D., Trembath, J., Brooke, J. K., Bart, M., et al. (2013). Optical properties of Saharan dust aerosol and contribution from the coarse mode as measured during the Fennec 2011 Aircraft Campaign. *Atmospheric Chemistry and Physics*, *13*, 303–325. https://doi.org/10.5194/acp-13-303-2013
Sagoo, N., & Storelvmo, T. (2017). Testing the sensitivity of past climates to the indirect effects of dust. *Geophysical Research Letters*, *44*, 5807–5817. https://doi.org/10.1002/2017GL072584
Sinyuk, A., Torres, O., & Dubovik, O. (2003). Combined use of satellite and surface observations to infer the imaginary part of refractive index of Saharan dust. *Geophysical Research Letters*, *30*(2), 1081. https://doi.org/10.1029/2002GL016189
Skinner, C., & Poulsen, C. (2016). The role of fall season tropical plumes in enhancing Saharan rainfall during the African humid period. *Geophysical Research Letters*, *43*, 349–358. https://doi.org/10.1002/2015GL066318
Sokolik, I., Andronova, A., & Johnson, T. (1993). Complex refractive index of atmospheric dust aerosols. *Atmospheric Environment*, *27A*, 2495–2502.
Solmon, F., Mallet, M., Elguindi, N., Giorgi, F., Zakey, A., & Konaré, A. (2008). Dust aerosol impact on regional precipitation over western Africa, mechanisms and sensitivity to absorption properties. *Geophysical Research Letters*, *35*, L24705. https://doi.org/10.1029/2008GL035900
Tierney, J., Pausata, F., & deMenocal, P. (2017). Rainfall regimes of the Green Sahara. *Science Advances*, *3*, e1601503.
Todd, M., Washing, R., Martins, J., Dubovik, O., Lizcano, G., M'Bainayel, S., & Engelstaedter, S. (2007). Mineral dust emission from the Bodélé depression, northern Chad, during BoDEx 2005. *Journal of Geophysical Research*, *112*, D06207. https://doi.org/10.1029/2006JD007170
Vamborg, F., Brovkin, V., & Claussen, M. (2011). The effect of a dynamic background albedo scheme on Sahel/Sahara precipitation during the mid-Holocene. *Climate of the Past*, *7*, 117–131.
Vellinga, M., Roberts, M., Luigi Vidale, P., Mizielinski, M., Demory, M.-E., Schiemann, R., et al. (2016). Sahel decadal rainfall variability and the role of model horizontal resolution. *Geophysical Research Letters*, *43*, 326–333. https://doi.org/10.1029/2015GL066690
Vogel, P., Knippertz, P., Fink, A., Andreas, S., & Tilmann, G. (2018). Skill of global raw and postprocessed ensemble predictions of rainfall over northern tropical Africa. *Weather and Forecasting*, *33*, 369–388.
Volz, F. (1973). Infrared optical constants of ammonium sulfate, Sahara dust, volcanic pumice and flyash. *Applied Optics*, *12*, 564–568.
Williams, R., McGee, D., Kinsley, C. W., Ridley, D. A., Hu, S., Fedorov, A., et al. (2016). Glacial to Holocene changes in trans-atlantic Saharan dust transport and dust-climate feedbacks. *Science Advances*, *2*, e1600445.
Woodward, S. (2001). Modeling the atmospheric life cycle and radiative impact of mineral dust in the Hadley Centre Climate Model. *Journal of Geophysical Research*, *106*(D16), 18,155–18,166.
Woodward, S. (2011). Mineral dust in HadGEM2 (*Hadley Centre Technical Note*). Exeter, UK: Met Office Hadley Centre for Climate Change.
Yoshioka, M., Mahowald, N. M., Conley, A. J., Collins, W. D., Fillmore, D. W., Zender, C. S., & Coleman, D. B. (2007). Impact of desert dust radiative forcing on Sahel precipitation: Relative Importance of dust compared to sea surface temperature variations, vegetation changes, and greenhouse gas warming. *Journal of Climate*, *20*, 1445–1467. https://doi.org/10.1175/JCLI4056.1
Zakey, A., Solmon, F., & Giorgi, F. (2006). Implementation and testing of a desert dust module in a regional climate model. *Atmospheric Chemistry and Physics*, *6*, 4687–4704.